Proton hot spots & exclusive vector meson production

Based on
S. Demirci, S. Schlichting & T. Lappi
Phys.Rev.D 106 (2022) 7, 074025

O. Garcia-Montero, Y. Hoffmann & S. Schlichting
arXiv:2511.22763 [hep-ph]

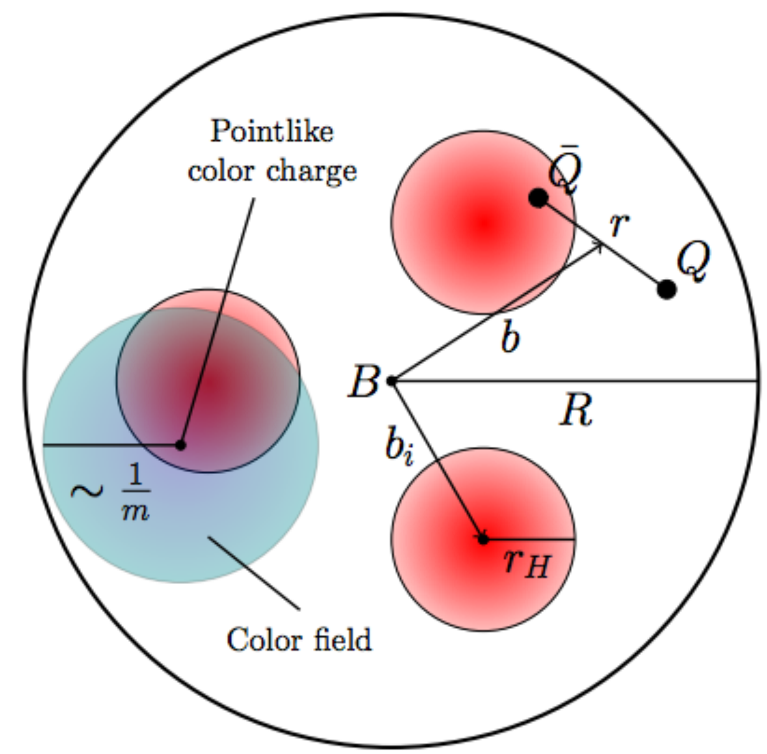

EMMI Workshop, GSI
July 2026

CRC-TR 211
Strong-interaction matter
under extreme conditions

UNIVERSITÄT
BIELEFELD

Scope/Motivation

Intrinsic interest to un-reaveal partonic many body structure of the proton beyond inclusive single-parton distributions

We want to understand…

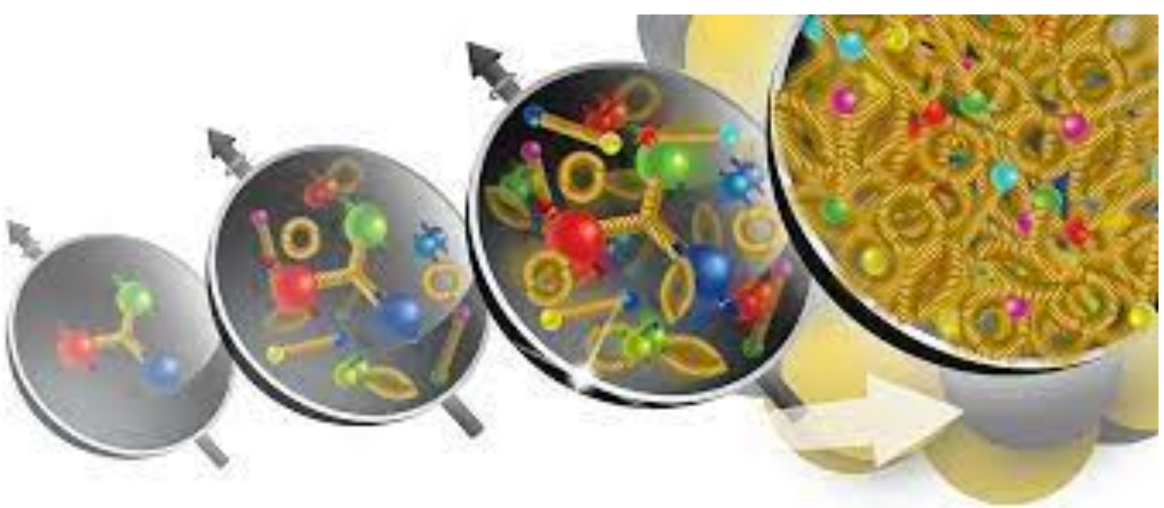

https://www.bnl.gov/eic/rhic-eic-comparison.php

..but we actually measure is …

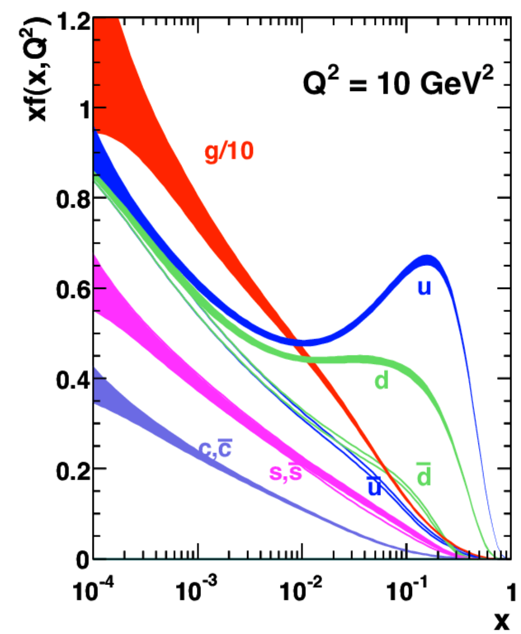

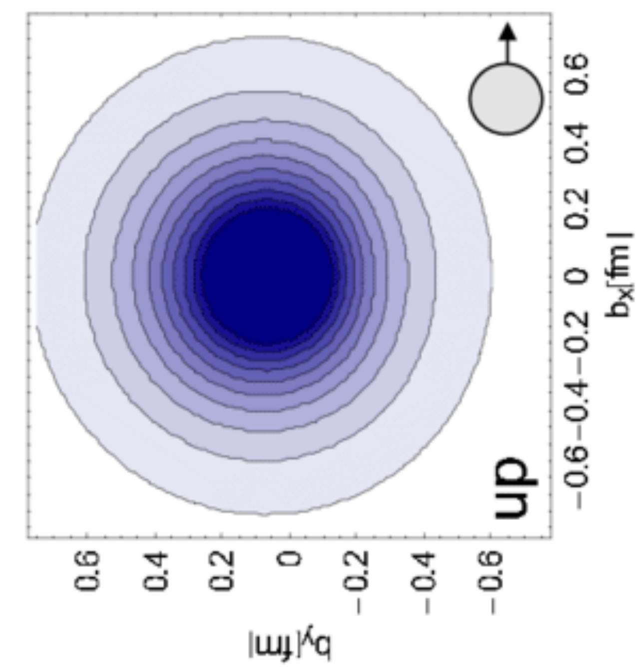

… so can we go beyond?

Necessity to understand correlations/fluctuations of proton structure for description of high-energy hadron collisions at RHIC and LHC

Flow in p+A

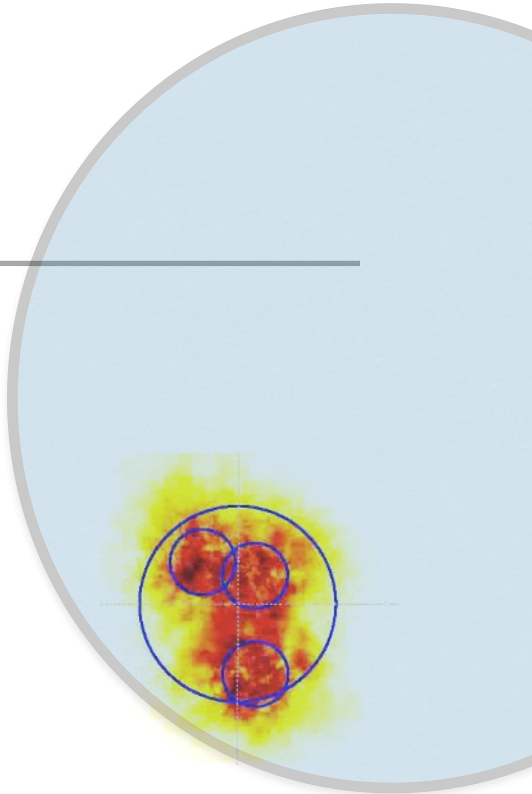

Collective flow observed in high-energy p+A collisions is geometrically driven by response to eccentricity (e_2) of initial state energy density

$$v_2 \sim k_{22}\, e_2$$

Event geometry reflects event-by-event fluctuations of the proton geometry

Schenke, Venugopalan PRL 113 (2014) 102301

Since response is not necessarily hydrodynamic in small systems, difficult to disentangle initial state eccentricity (e_2) and final state response (v_2/e_2) from p+A collisions alone

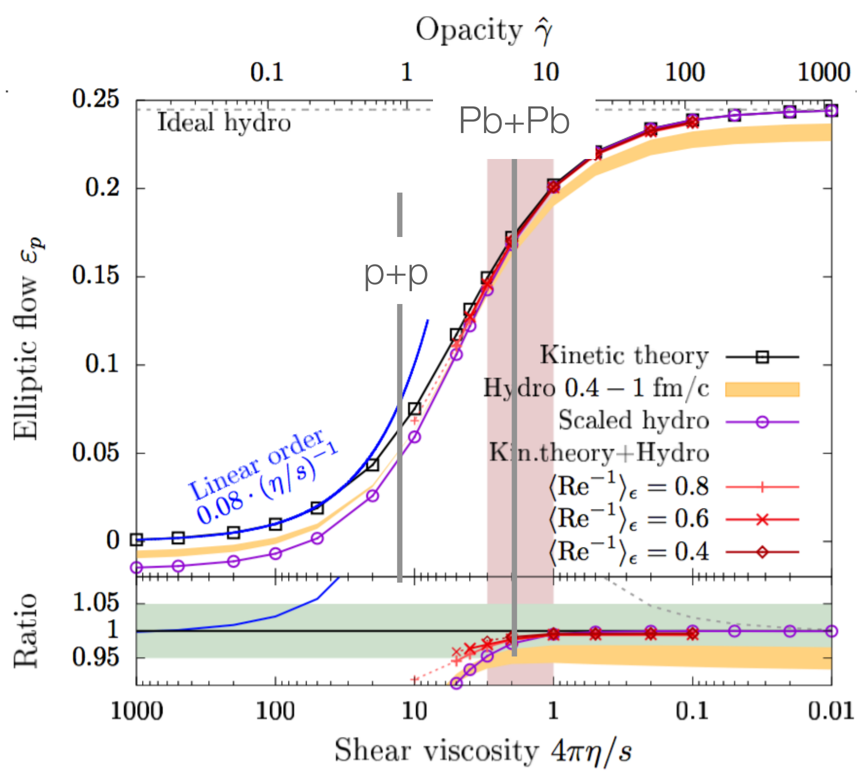

Ambrus, SS, Werthmann
PRL 130 (2023) 15, 152301

Methodology

Within Color-Glass Condensate effective theory of high-energy QCD can describe p+A and e+A collisions on the same footing

Goal: Develop simple (mostly analytically tractable) model of fluctuating proton structure to investigate

- constraining power of exclusive $\gamma^{*}+p \to J/\psi+p^{(*)}$ vector meson production
- sensitivity of p+A geometry to different aspects of proton structure

Similar works by Schenke, Mäntysaari, Salazar and Kumar, Toll

Fluctuating proton model

Color-charge density concentrated around

N_q hot spots

Size of hot-spot r_H (Gaussian)

color field of each charge extends up to

IR regulator 1/m

Individual hot-spots distributed within

Size R of proton (Gaussian)

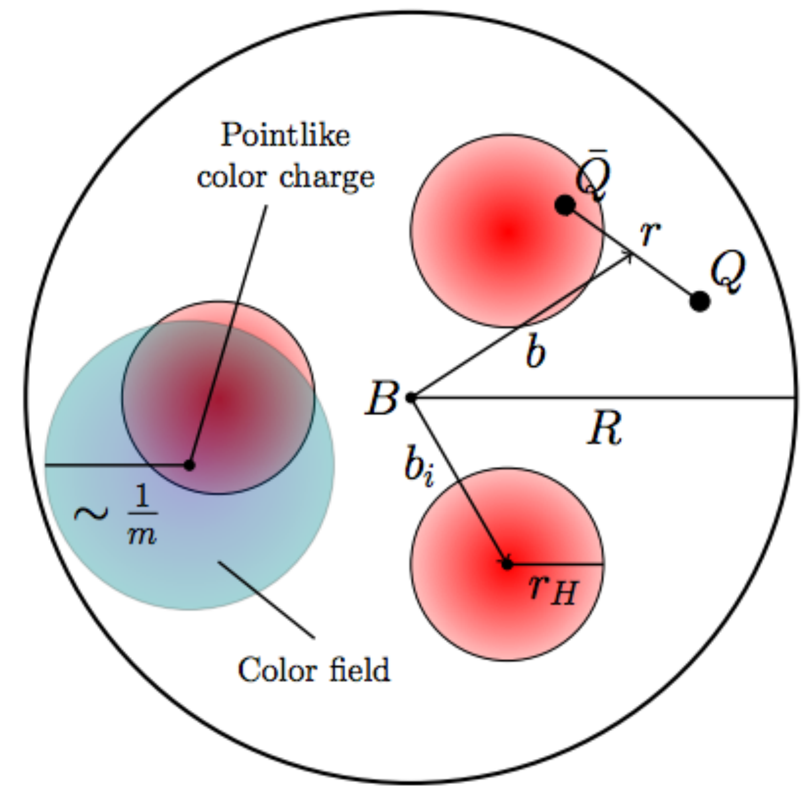

different hot-spots uncorrelated, except for center-of-mass constraint

We will adopt ``dilute'' approximation (leading-twist) to make calculation analytically feasible and compare to numerical calculations in "dense" case to study saturation effects

Fluctuating proton model

Color-charge density concentrated around N_q hot-spots

$$\langle \rho^a(\mathbf{x})\rho^b(\mathbf{y})\rangle_{CGC} = \sum_{i=1}^{N_q} \mu^2\left(\frac{\mathbf{x}+\mathbf{y}}{2} - \mathbf{b}_i\right)\delta^{(2)}(\mathbf{x}-\mathbf{y})\delta^{ab},$$

$$\mu^2(\mathbf{x}) = \frac{\mu_0^2}{2\pi r_H^2}\exp\left[-\frac{\mathbf{x}^2}{2r_H^2}\right],$$

Individual hot-spots distributed according to $T(\mathbf{b}) = \frac{1}{2\pi R^2}\exp\left[-\frac{\mathbf{b}^2}{2R^2}\right].$

Different hot-spots uncorrelated, except for center-of-mass constraint

$$\langle\langle \mathcal{O}\rangle\rangle = \left(\frac{2\pi R^2}{N_q}\right)\int \prod_{i=1}^{N_q}\left[\mathrm{d}^2\mathbf{b}_i T(\mathbf{b}_i - \mathbf{B})\right]\delta^{(2)}\left(\frac{1}{N_q}\sum_{i=1}^{N_q}\mathbf{b}_i - \mathbf{B}\right)\langle \mathcal{O}\rangle_{CGC},$$

Double average includes CGC average over color charge fluctuations and average over location of hot-spots

Vector meson production in DIS

Exclusive production of QQ vector meson in γ^*+p-> J/ψ+p$^{(*)}$

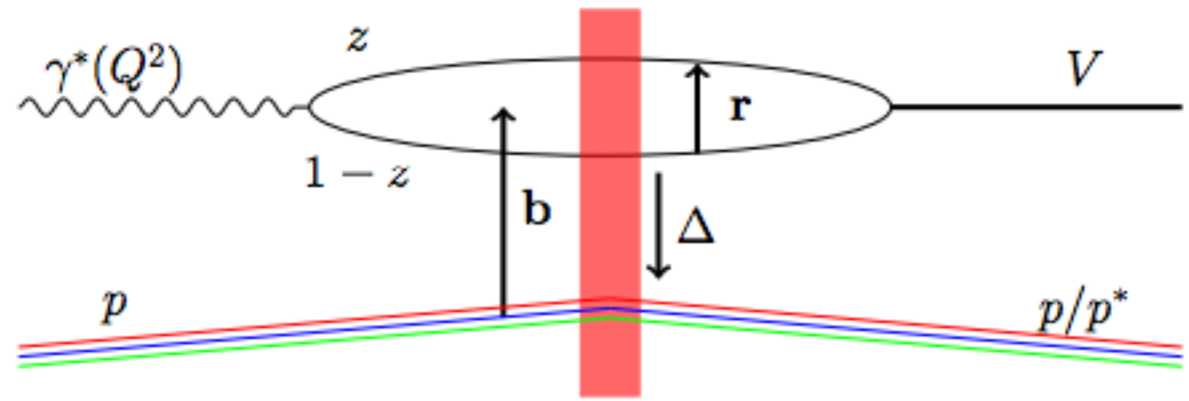

Scattering amplitude at LO in small-x limit given by

$$\mathcal{A}_{T,L}^{\gamma^* p \to Vp}(Q^2,\Delta) = i \int d^2\mathbf{r} \int d^2\mathbf{b} \int \frac{dz}{4\pi} (\Psi^*\Psi_V)_{T,L}(Q^2,\mathbf{r},z) \exp\left\{-i\left[\mathbf{b} + \left(\frac{1}{2}-z\right)\mathbf{r}\right]\cdot\Delta\right\} \frac{d\sigma_{\mathrm{dip}}^{\mathrm{p}}}{d^2\mathbf{b}}(\mathbf{b},\mathbf{r}).$$

Distinguish coherent/incoherent production

$$\frac{d\sigma_{T,L}^{\gamma^* p \to Vp}}{dt} = \frac{1}{16\pi} |\langle\langle \mathcal{A}_{T,L}^{\gamma^* p \to Vp}(Q^2,\Delta)\rangle\rangle|^2$$

$$\frac{d\sigma_{T,L}^{\gamma^* p \to Vp^*}}{dt} = \frac{1}{16\pi}\left(\langle\langle |\mathcal{A}_{T,L}^{\gamma^* p \to Vp}(Q^2,\Delta)|^2\rangle\rangle - |\langle\langle \mathcal{A}_{T,L}^{\gamma^* p \to Vp}(Q^2,\Delta)\rangle\rangle|^2\right).$$

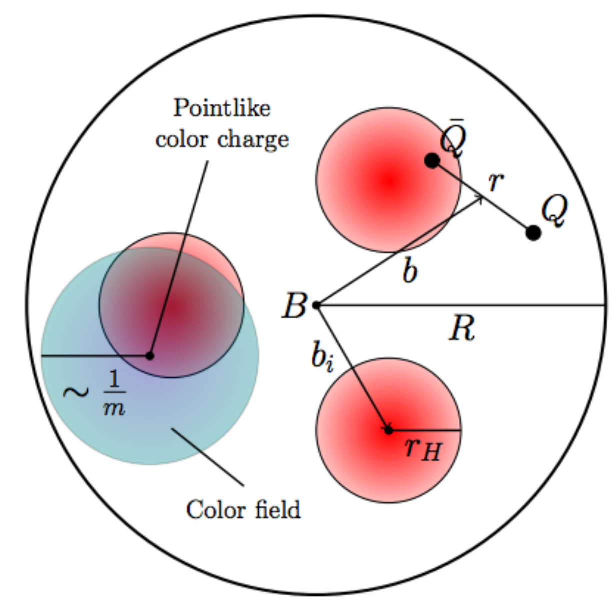

which probe directly average/fluctuations of dipole cross section

Vector meson production in DIS

Non-relativistic limit of QQ wave function

$$(\Psi_V^* \Psi_\gamma)_T = -A_Q \sqrt{2 m_Q N_c} e_Q e K_0(\varepsilon |\mathbf{r}|) \delta \left(z - \frac{1}{2} \right)$$

Dipole cross-section

$$\frac{d\sigma_{\mathrm{dip}}^{\mathrm{p}}}{d^2\mathbf{b}}(\mathbf{b}, \mathbf{r}) = 2\, \frac{1}{N_c} \mathrm{tr} \left[1 - V(\mathbf{x}) V^\dagger(\mathbf{y}) \right]$$

$$V(\mathbf{x}) = \mathcal{P}_+ \exp \left[ig \int_{-\infty}^{\infty} dz^+ \int d^2\mathbf{z} G(\mathbf{x} - \mathbf{z}) \rho_a(z^+, \mathbf{z}) t^a \right].$$

Dilute limit: Expanded to leading non-trivial order in rho's to allow for as much analytical control as possible

Saturation effects: Numerical evaluation of non-linearly evaluated multipole correlators

Vector meson production in DIS — Dilute

Coherent cross-section

$$\frac{d\sigma_{T,L}^{\gamma^* p\to Vp}}{dt} = \frac{C_{T,L}^2}{16\pi}\frac{g^4\mu_0^4(N_c^2-1)^2N_q^2}{(2\pi N_c)^2}$$
$$\times \exp\left(-\left[r_H^2+\left(\frac{N_q-1}{N_q}\right)R^2\right]\Delta^2\right) Z(\Delta,m^2,\varepsilon')^2.$$

show exponential decay with coh. radius modulated by Z-function
which characterizes structure of QQ-dipole and interaction
with color charges

$$Z(\Delta,m^2,\varepsilon') \equiv \int d^2\mathbf{r}K_0(\varepsilon'|\mathbf{r}|)$$
$$\times\left\{\cos\left(\frac{1}{2}\Delta\cdot\mathbf{r}\right)\Psi\left(0,\Delta,m^2\right)-\Psi(\mathbf{r},\Delta,m^2)\right\}$$

$$\Psi\left(\mathbf{r},\Delta,m^2\right)=\int_0^{\frac{1}{2}} d\lambda\cos\left(\lambda\Delta\cdot\mathbf{r}\right)$$
$$\times\frac{|\mathbf{r}|K_1\left(|\mathbf{r}|\sqrt{-\Delta^2\lambda^2+\frac{1}{4}\Delta^2+m^2}\right)}{\sqrt{-\Delta^2\lambda^2+\frac{1}{4}\Delta^2+m^2}},$$

can be evaluated analytically in the limit m_Q >> all other scales
where dipole size **r** is truly small

Vector meson production in DIS — Dilute

Incoherent cross-section broken up into contributions from one/two hot-spots & with disconnected/connected color structure

$$\frac{d\sigma_{T,L}^{\gamma^* p\to V p^*}}{dt} = \left.\frac{d\sigma_{T,L}^{\gamma^* p\to V p^*}}{dt}\right|_{1,DC} + \left.\frac{d\sigma_{T,L}^{\gamma^* p\to V p^*}}{dt}\right|_{2,DC} + \left.\frac{d\sigma_{T,L}^{\gamma^* p\to V p^*}}{dt}\right|_{1,C} + \left.\frac{d\sigma_{T,L}^{\gamma^* p\to V p^*}}{dt}\right|_{2,C},$$

Hot-spot fluctuations

Color charge fluctuations

Hot-spot fluctuations: Same structure as coh. cross-section

$$\left.\frac{d\sigma_{T,L}^{\gamma^* p\to V p^*}}{dt}\right|_{1,DC} = \frac{C_{T,L}^2}{16\pi}\frac{g^4\mu_0^4(N_c^2-1)^2}{(2\pi N_c)^2}N_q\left[\exp\left(-\Delta^2 r_H^2\right) - \exp\left(-\left[r_H^2 + \left(\frac{N_q-1}{N_q}\right)R^2\right]\Delta^2\right)\right] Z(\Delta, m^2, \varepsilon')^2$$

Color charge fluctuations: Exhibit different structure and suppressed by ~1/N_c

$$\left.\frac{d\sigma_{T,L}^{\gamma^* p\to V p^*}}{dt}\right|_{1,C} = \frac{C_{T,L}^2}{16\pi}\frac{g^4\mu_0^4(N_c^2-1)}{2\pi^2 N_c^2}N_q K(r_H^2, \Delta, m^2, \varepsilon'^2)$$

with no factorization between structure of projectile and target

Vector meson production in DIS

Strikingly simple picture in truly non-relativistic limit $m_Q = m_t$

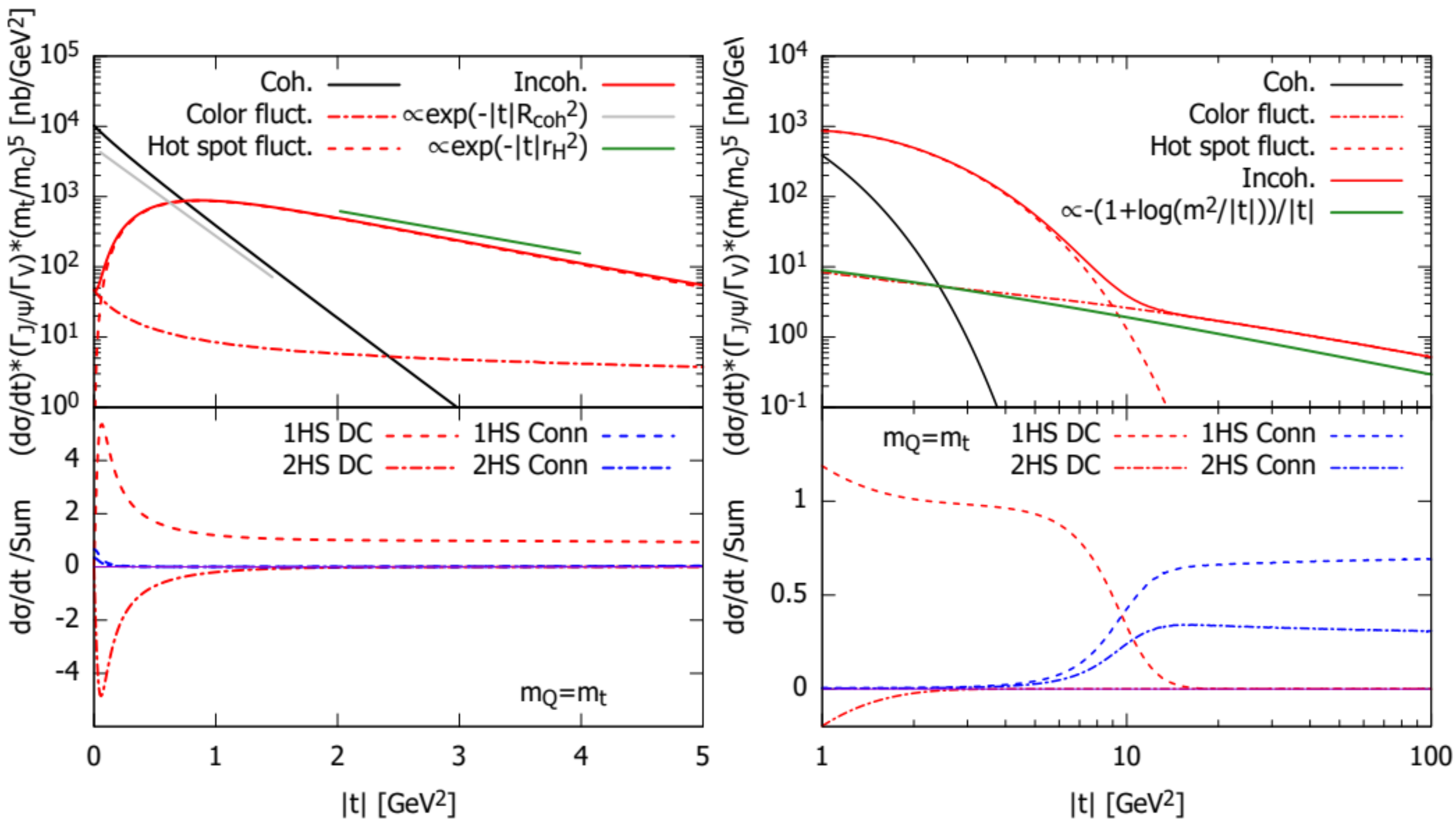

Vector meson production in DIS

Significantly larger sensitivity to structure of the probe for m_Q=m_c,m_b

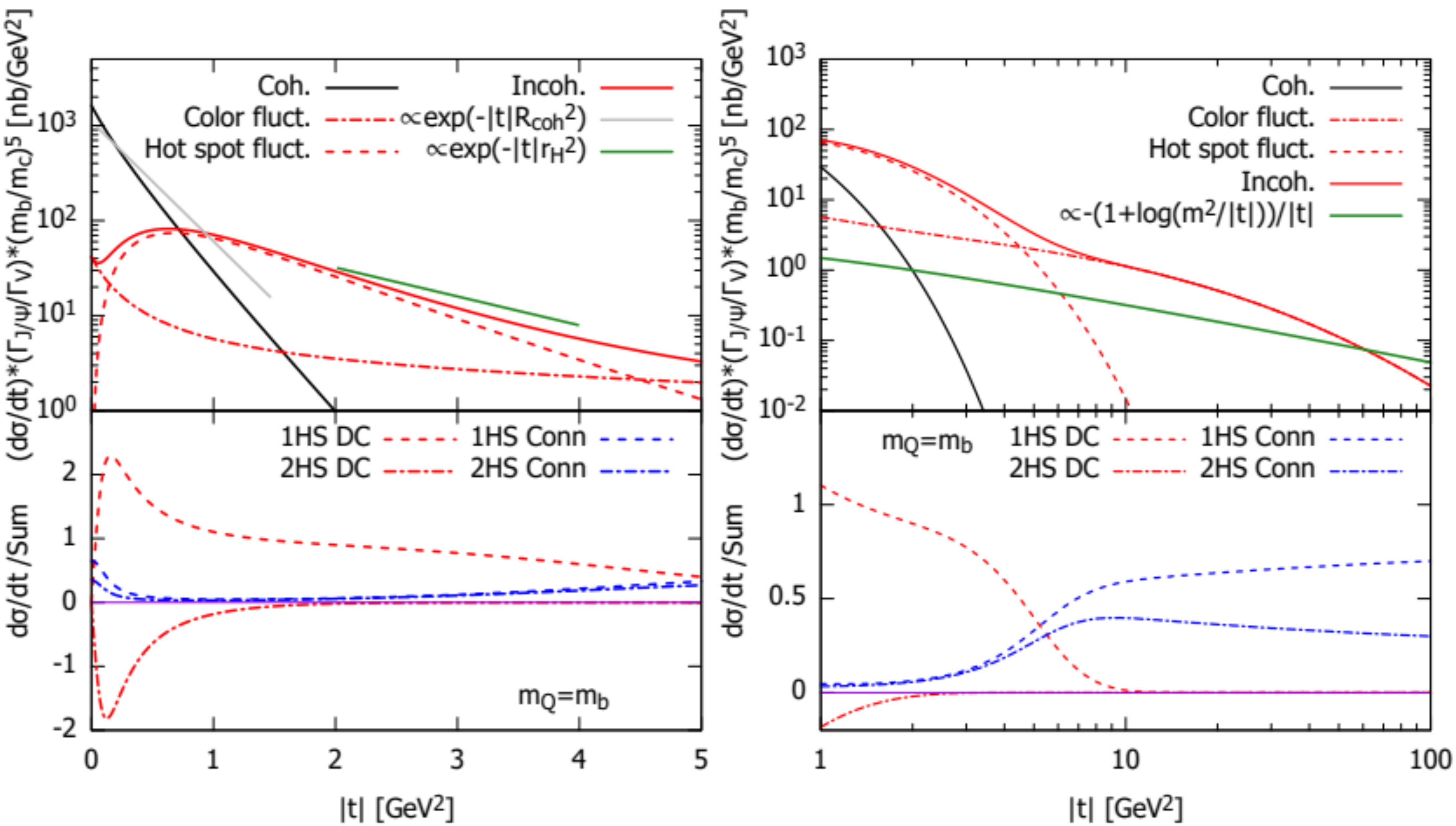

slopes no longer reflect proton/hot-spot size

Vector meson production in DIS

Significantly larger sensitivity to structure of the probe for $m_Q=m_c,m_b$

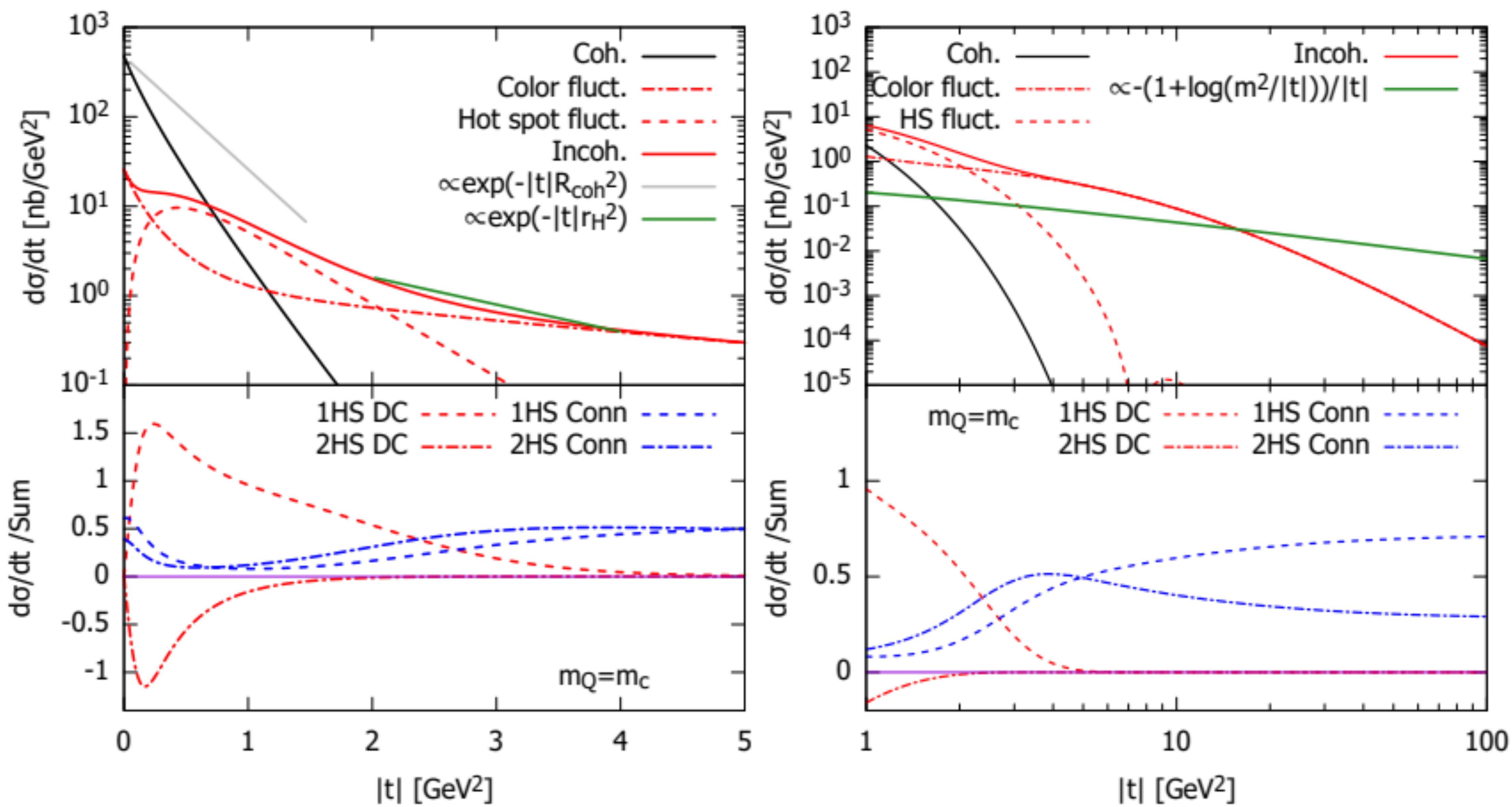

slopes no longer reflect proton/hot-spot size

Vector meson production in DIS— Dilute

Good description of t-dependence of HERA over large t range but relative normalization of coh. vs. incoherent off by a factor of 2.5

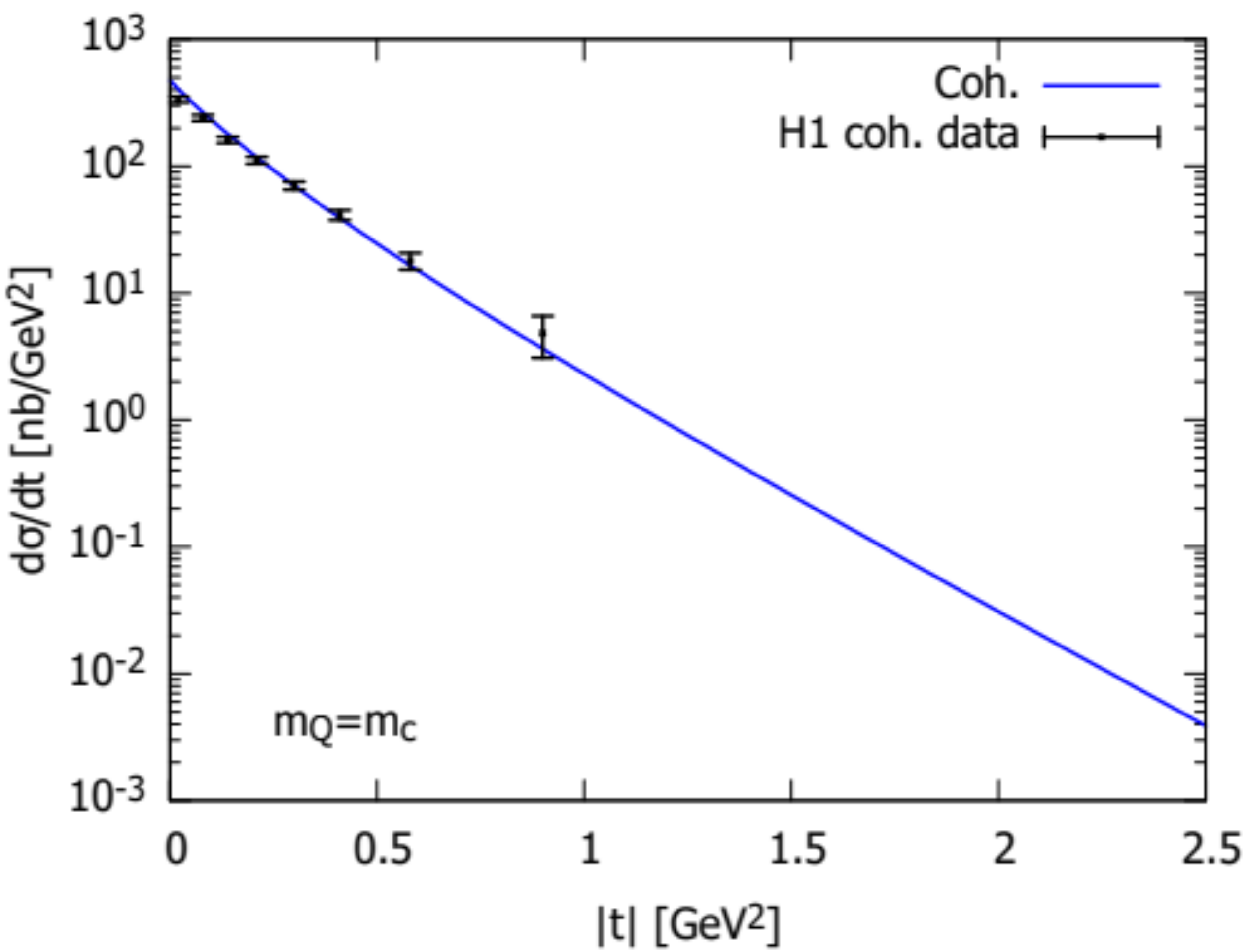

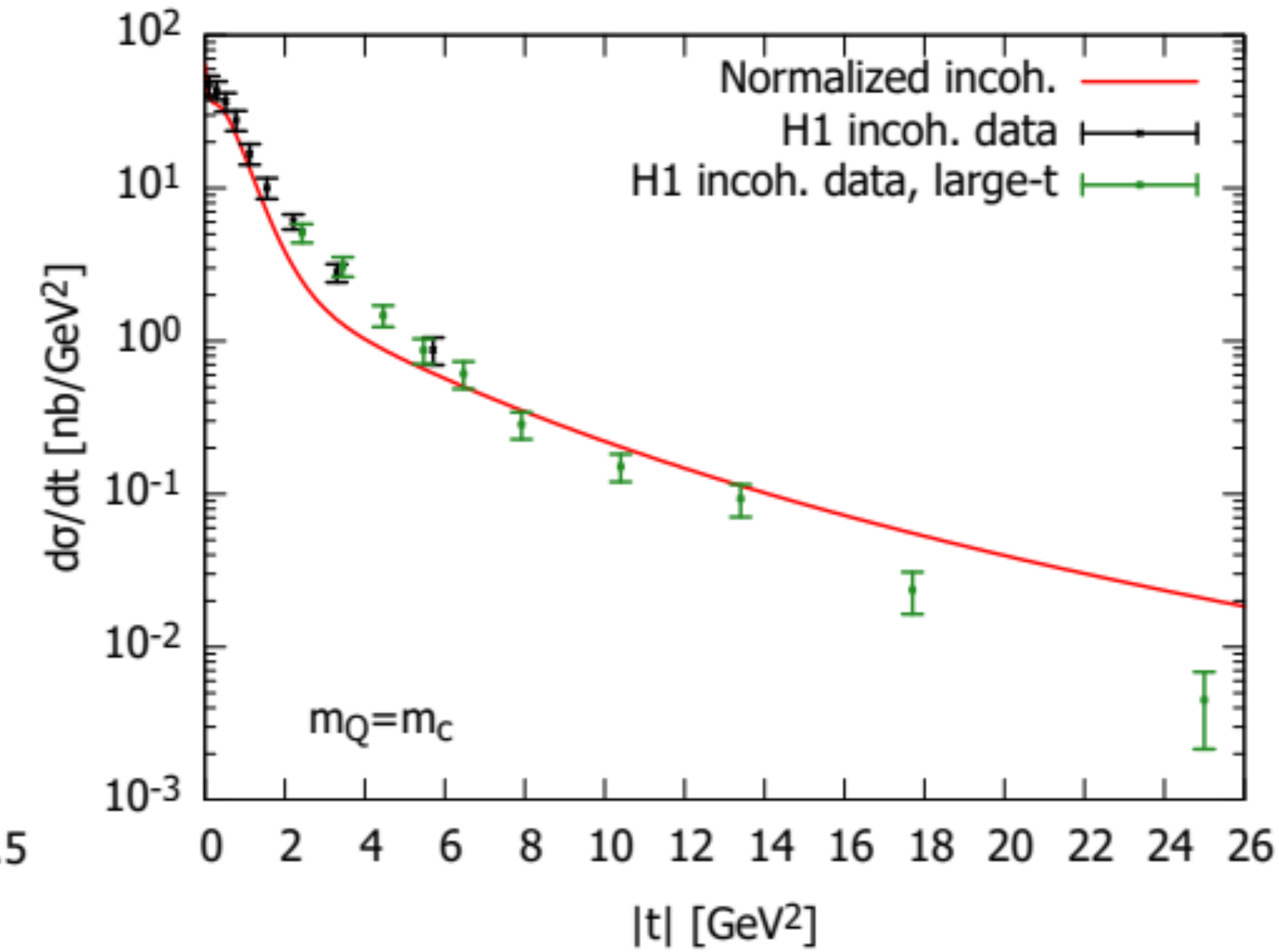

Hence no attempt to fit, but instead consider reasonable values to study anatomy of the cross-section

Vector meson production in DIS— Dense

Event-by-event Monte-Carlo sampling of hot-spot positions

Numerical evaluation of non-linear cross-section formula
 to include saturation effects

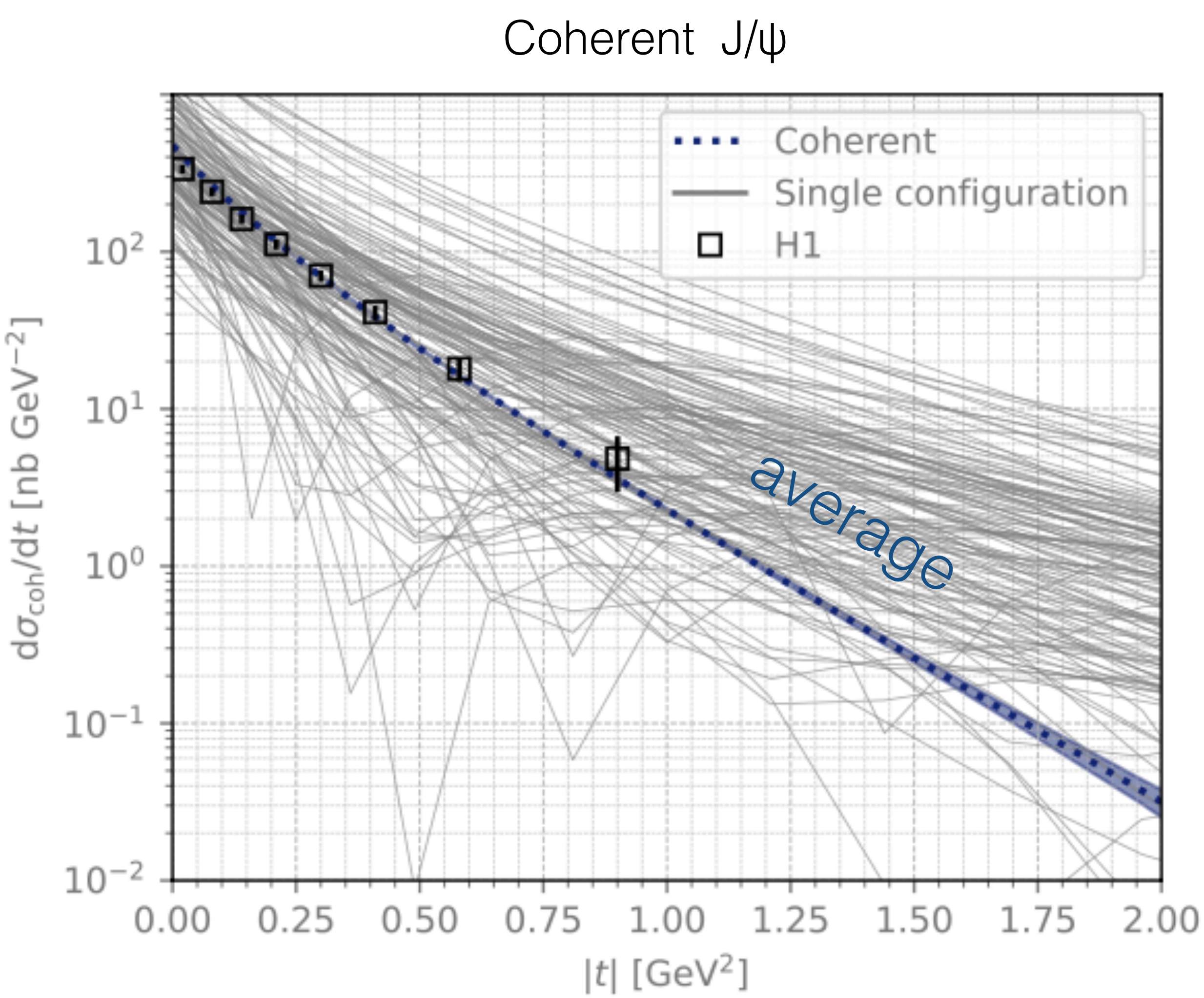

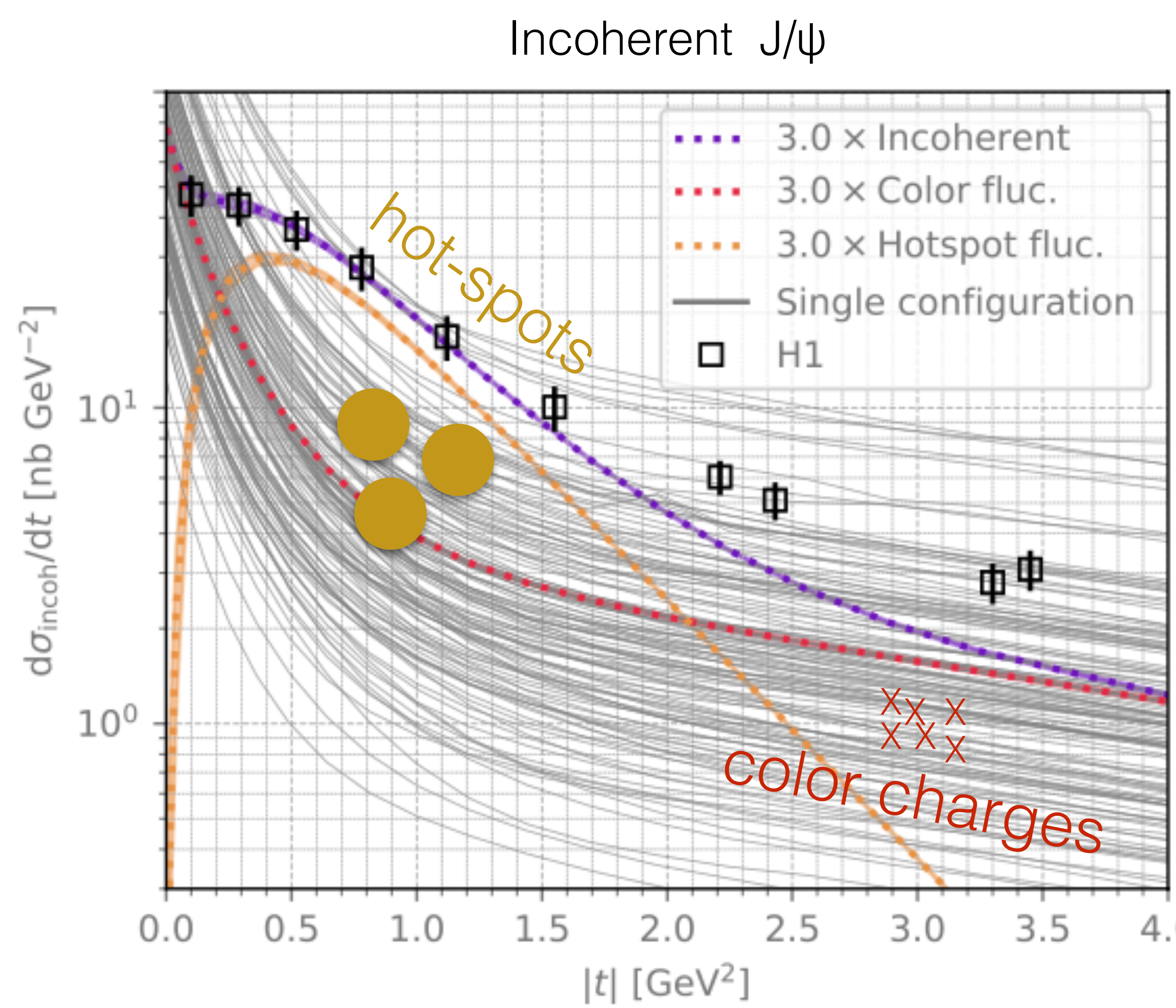

Saturation effects

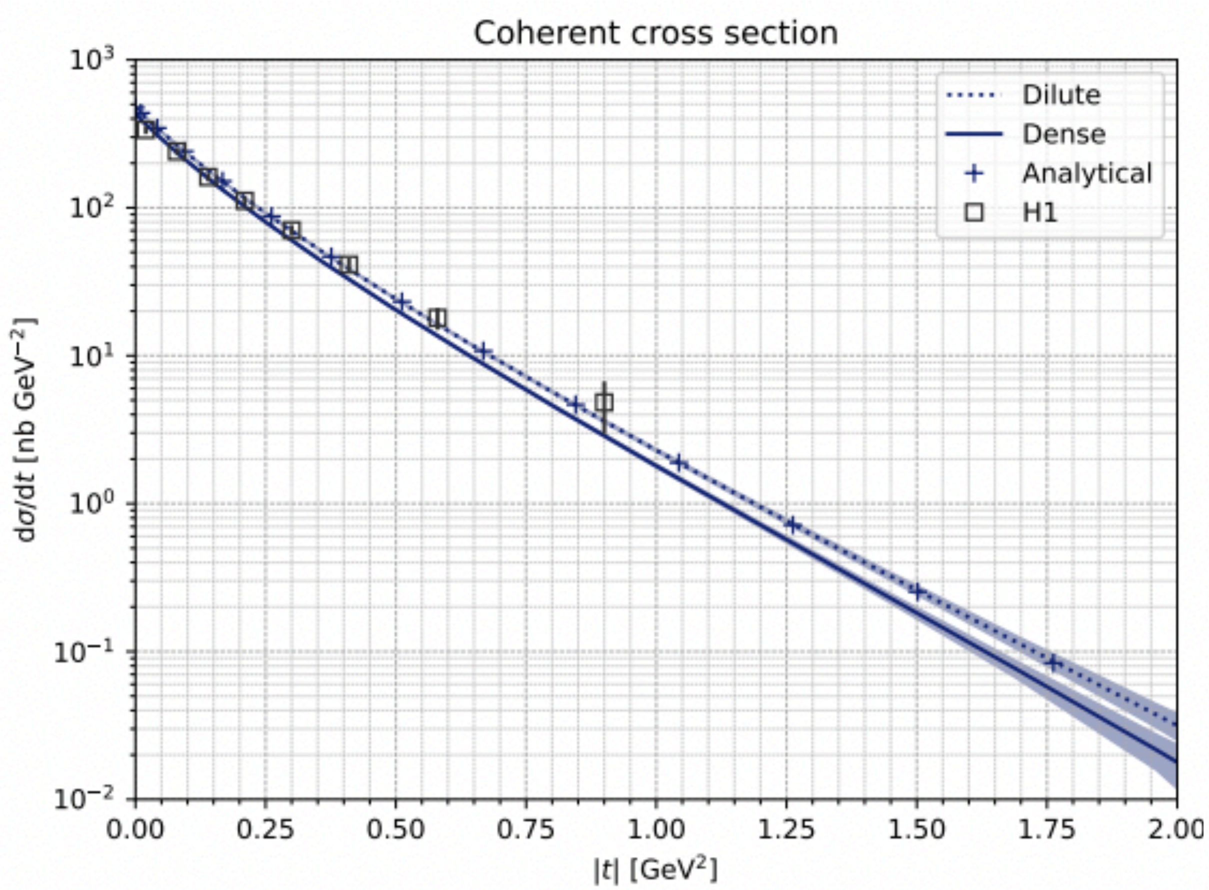

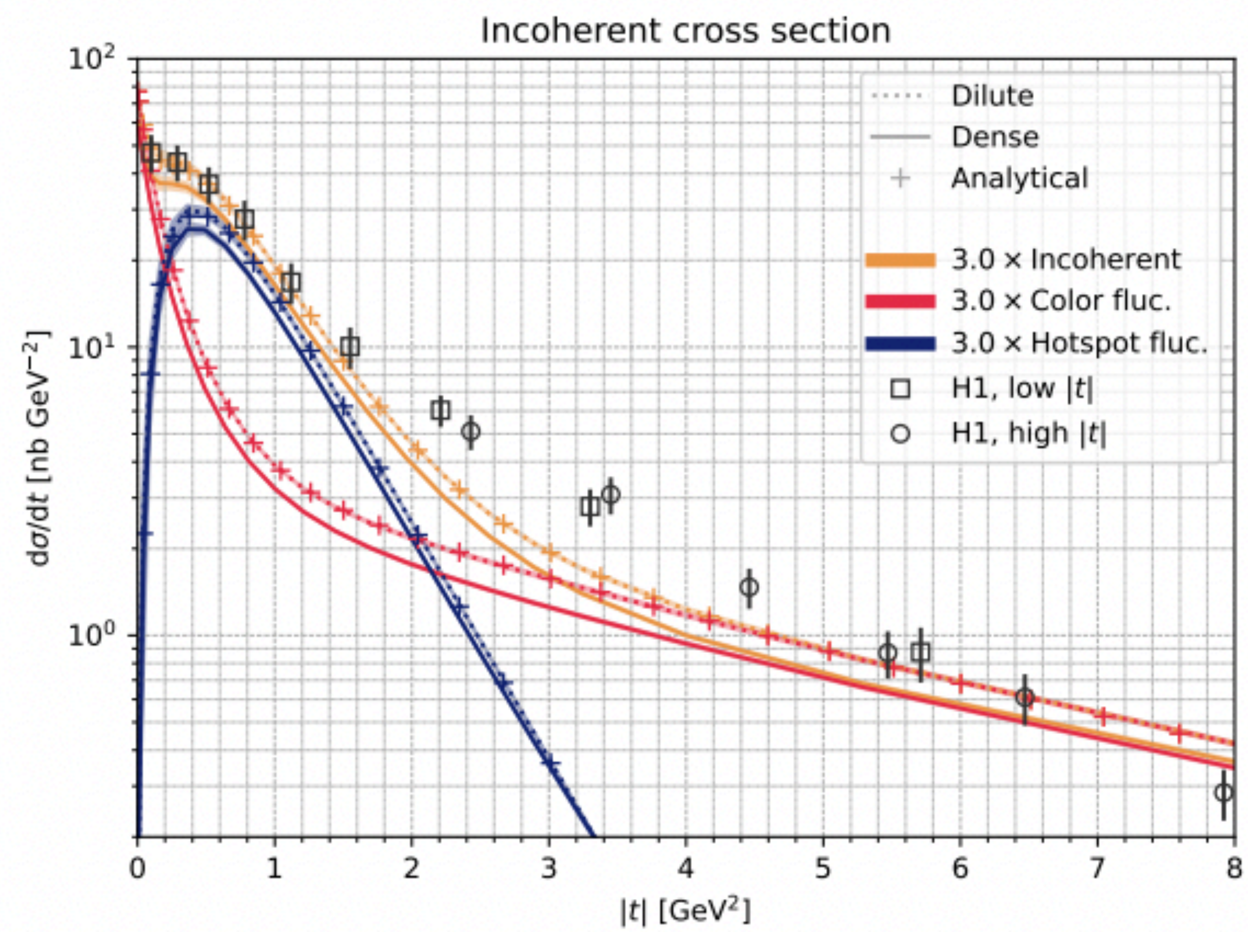

Suppression of the cross-section due to saturation effects, which is fairly uniform across entire t range for DIS on protons

Saturation effects

Enhancing saturation effects by increasing color charge density (smaller x, larger nuclei)

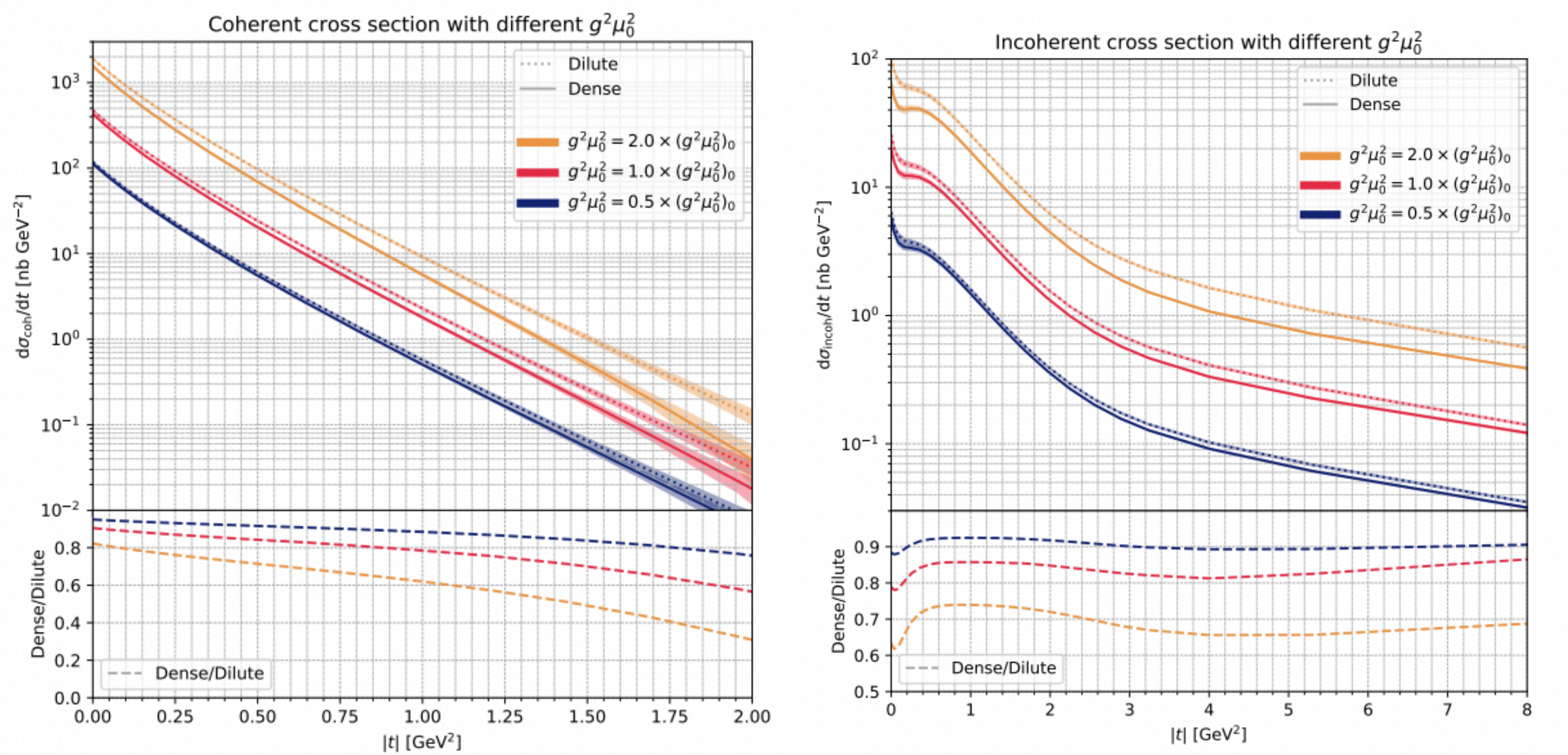

Simultaneous analysis of e/p/A+A

Simultaneous analysis of DIS and heavy-ion data can be used to constrain cold and hot QCD properties

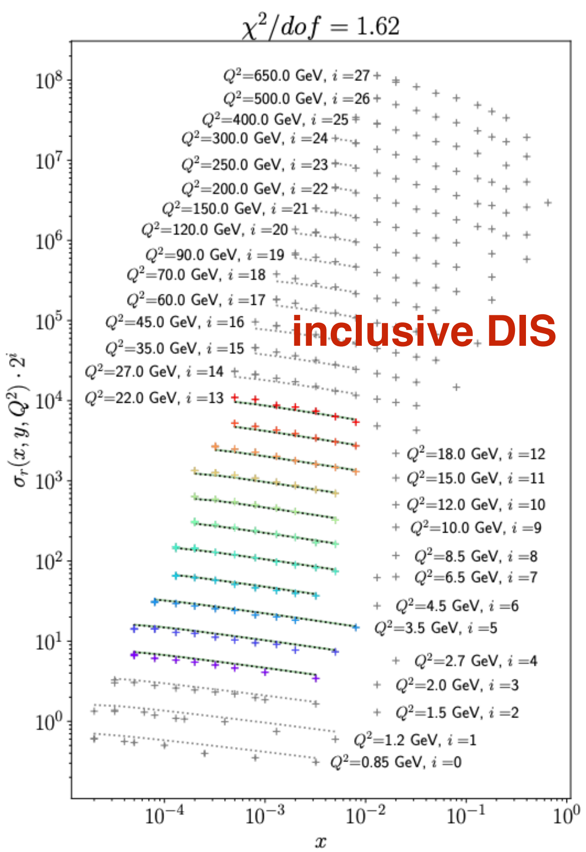

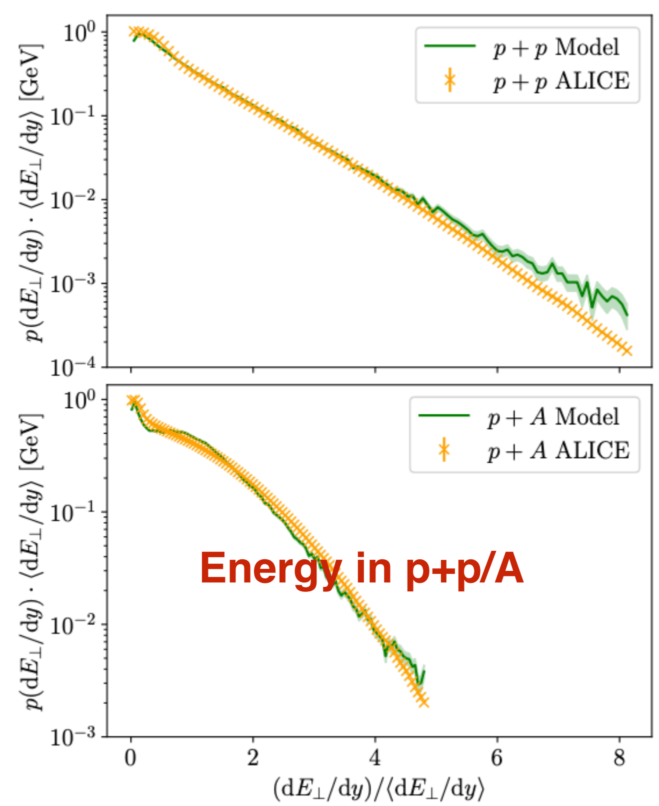

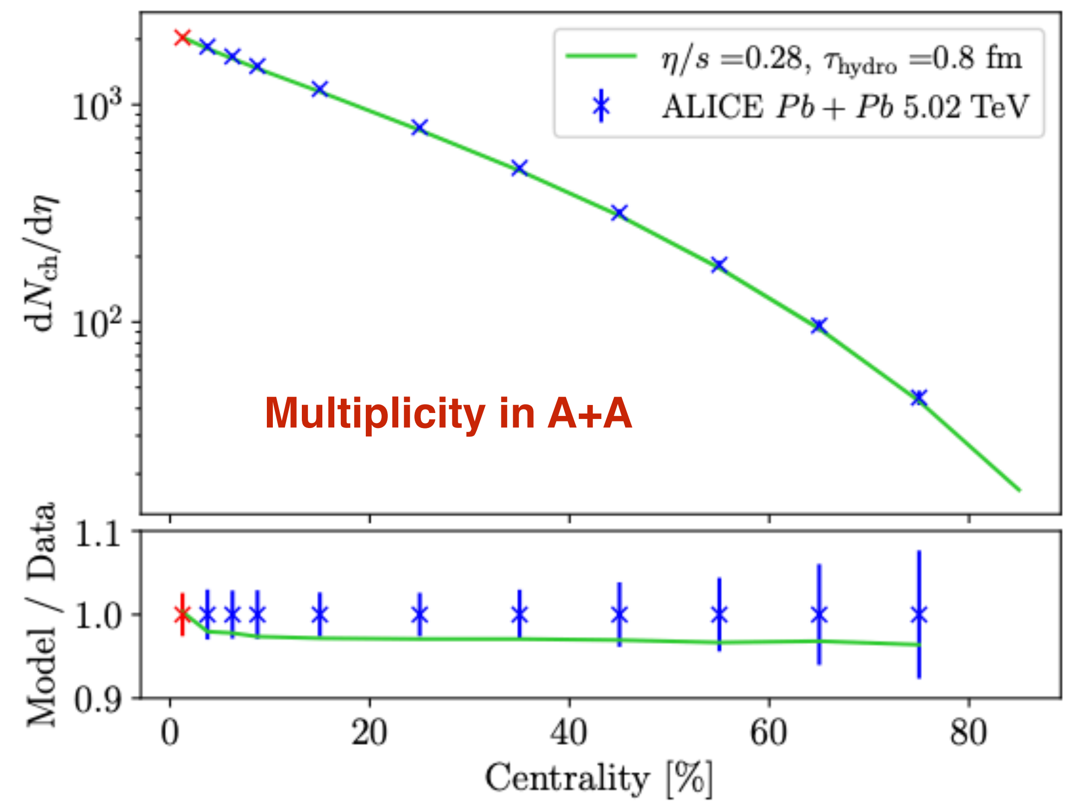

Proof-of-principle study for GBW model

Parameter	$\gamma^* + p$	$p+p/p+A$	$A+A$
$Q_{s,0}$	✓	✓	✓
λ	✓	✓	✓
δ	(✓)	(✓)	(✓)
σ_Q	(✓)	(✓)	(✓)
K		✓	✓
η/s			✓

``Constraining hot and cold nuclear matter properties from heavy-ion collisions and deep-inelastic scattering''
Andronic, Borghini, Du, Klein-Bösing, Krupczak, SS, arXiv:2504.02726

Eccentricities in p+A collisions

Explicit verification that “proton shape” fluctuations dominate eccentricity

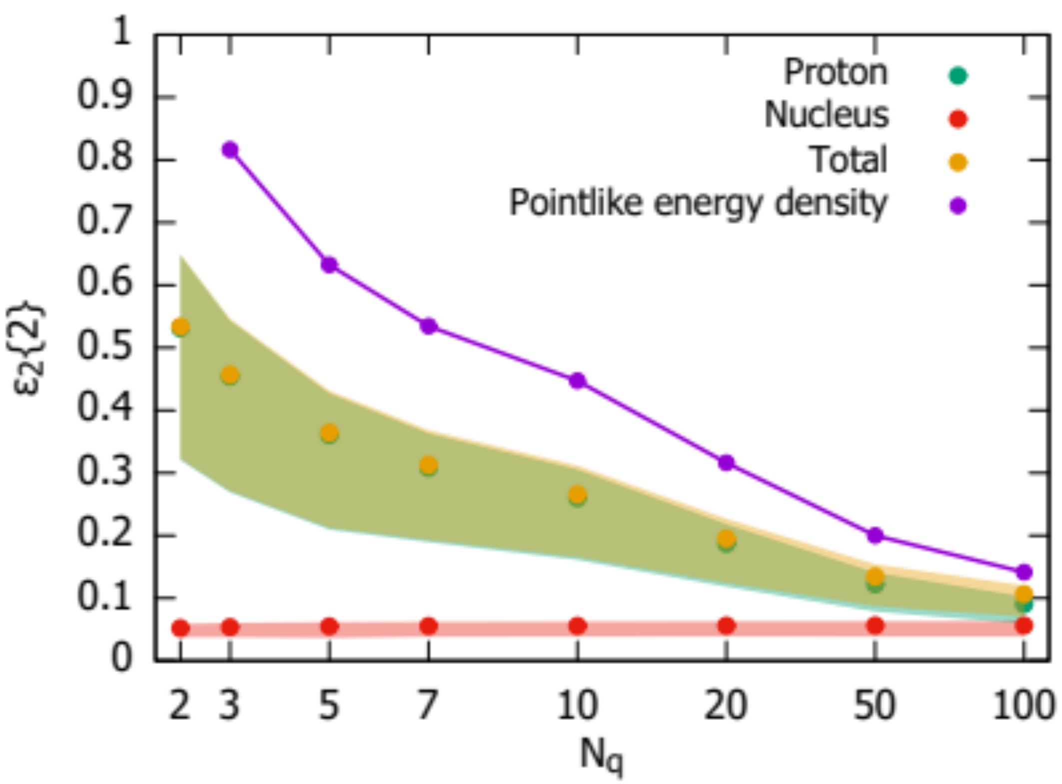

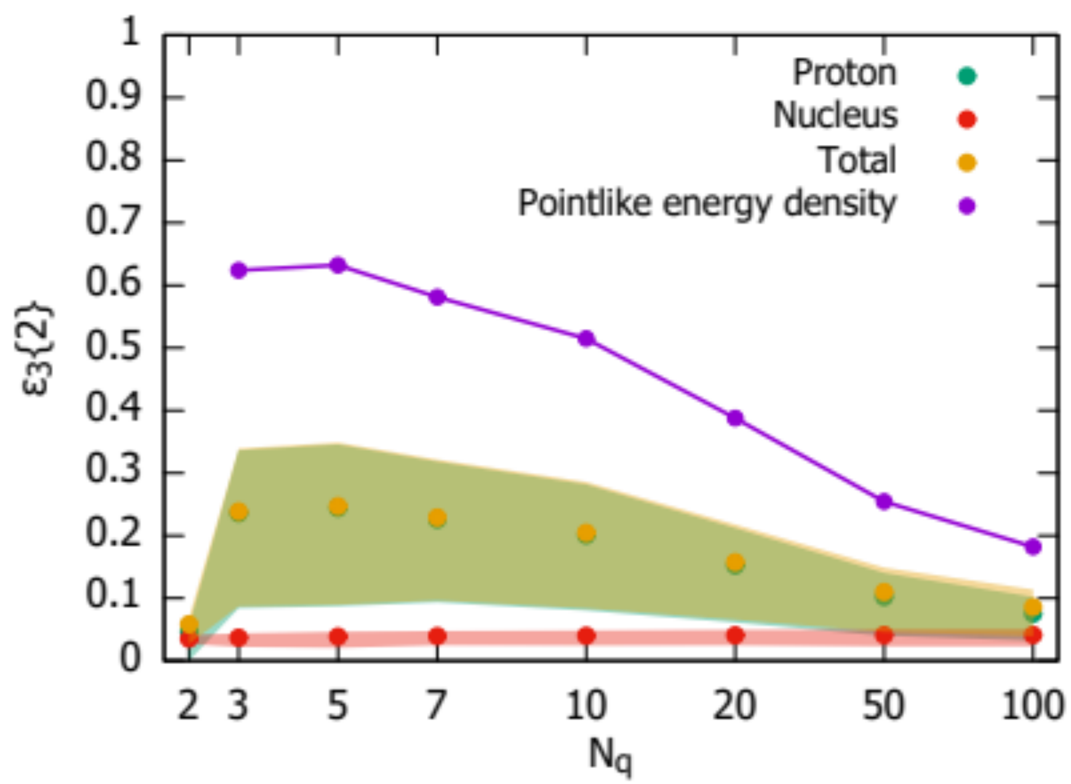

S. Demirci, S. Schlichting & T. Lappi Phys.Rev.D 103 (2021) 9, 094025

Strong sensitivity of eccentricities to

- IR regulator m (bands show 50% variations)
- Number of hot spots N_q

Simultaneous analysis of e/p/A+A

Simultaneous analysis of DIS and heavy-ion data can be used to constrain cold and hot QCD properties

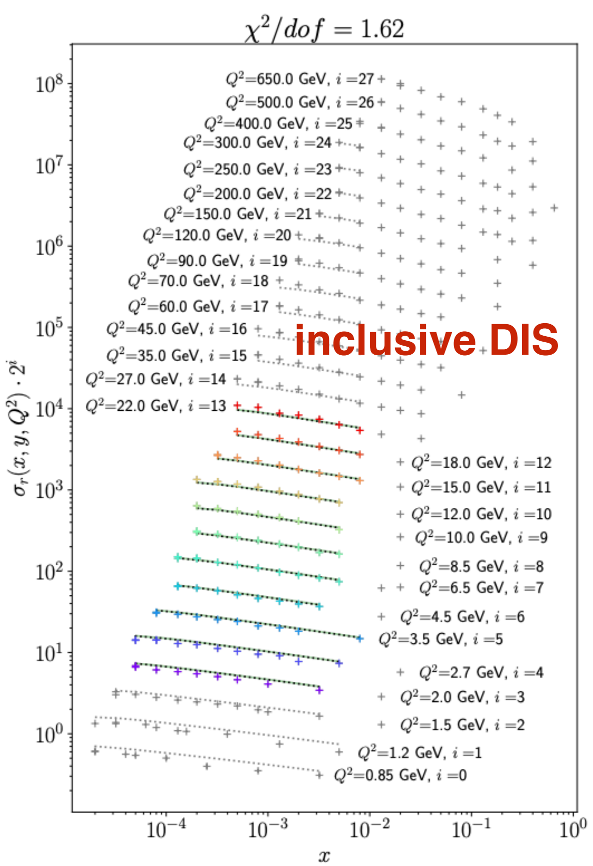

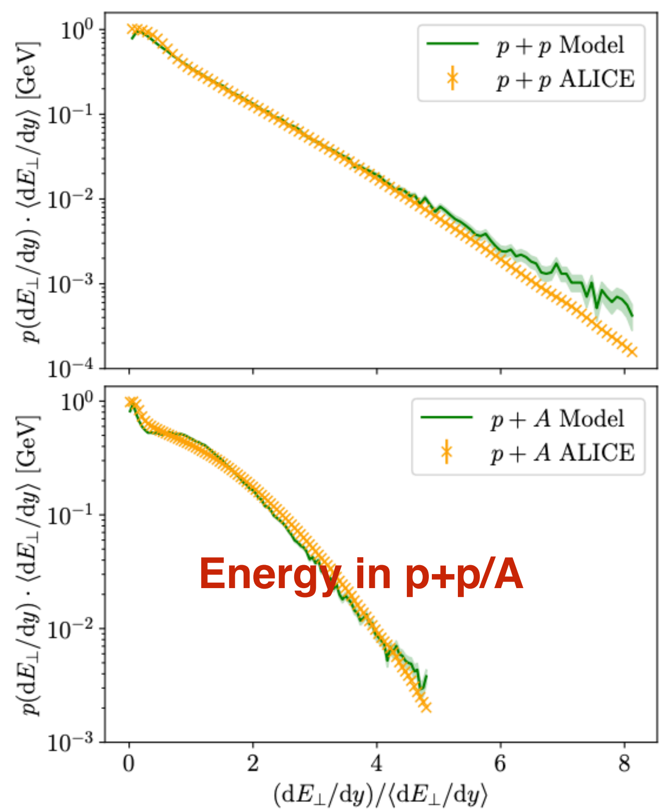

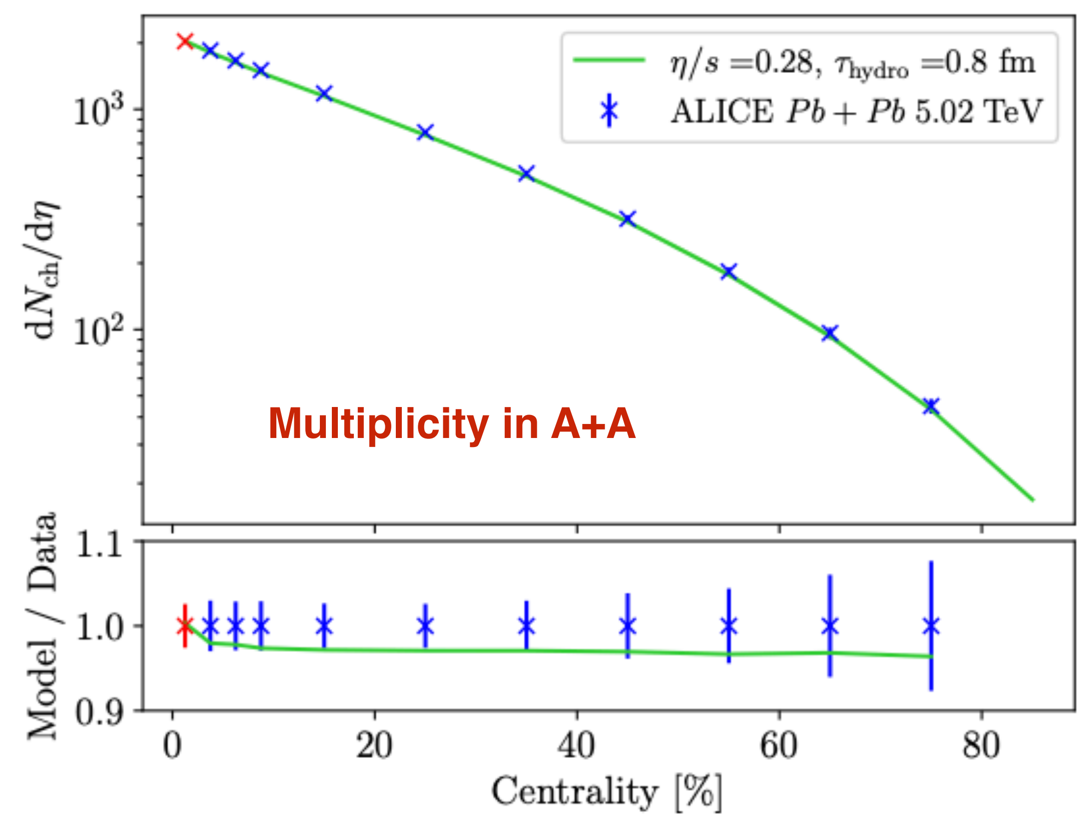

Proof-of principle study using impact parameter dependent GBW model

Parameter	$\gamma^* + p$	$p+p/p+A$	$A+A$
$Q_{s,0}$	✓	✓	✓
λ	✓	✓	✓
δ	(✓)	(✓)	(✓)
σ_Q	(✓)	(✓)	(✓)
K		✓	✓
η/s			✓

``Constraining hot and cold nuclear matter properties from heavy-ion collisions and deep-inelastic scattering'' Andronic, Borghini, Du, Klein-Bösing, Krupczak, SS, arXiv:2504.02726

Simultaneous analysis of e/p/A+A

Simultaneous analysis of DIS and heavy-ion data can be used to constrain cold and hot QCD properties

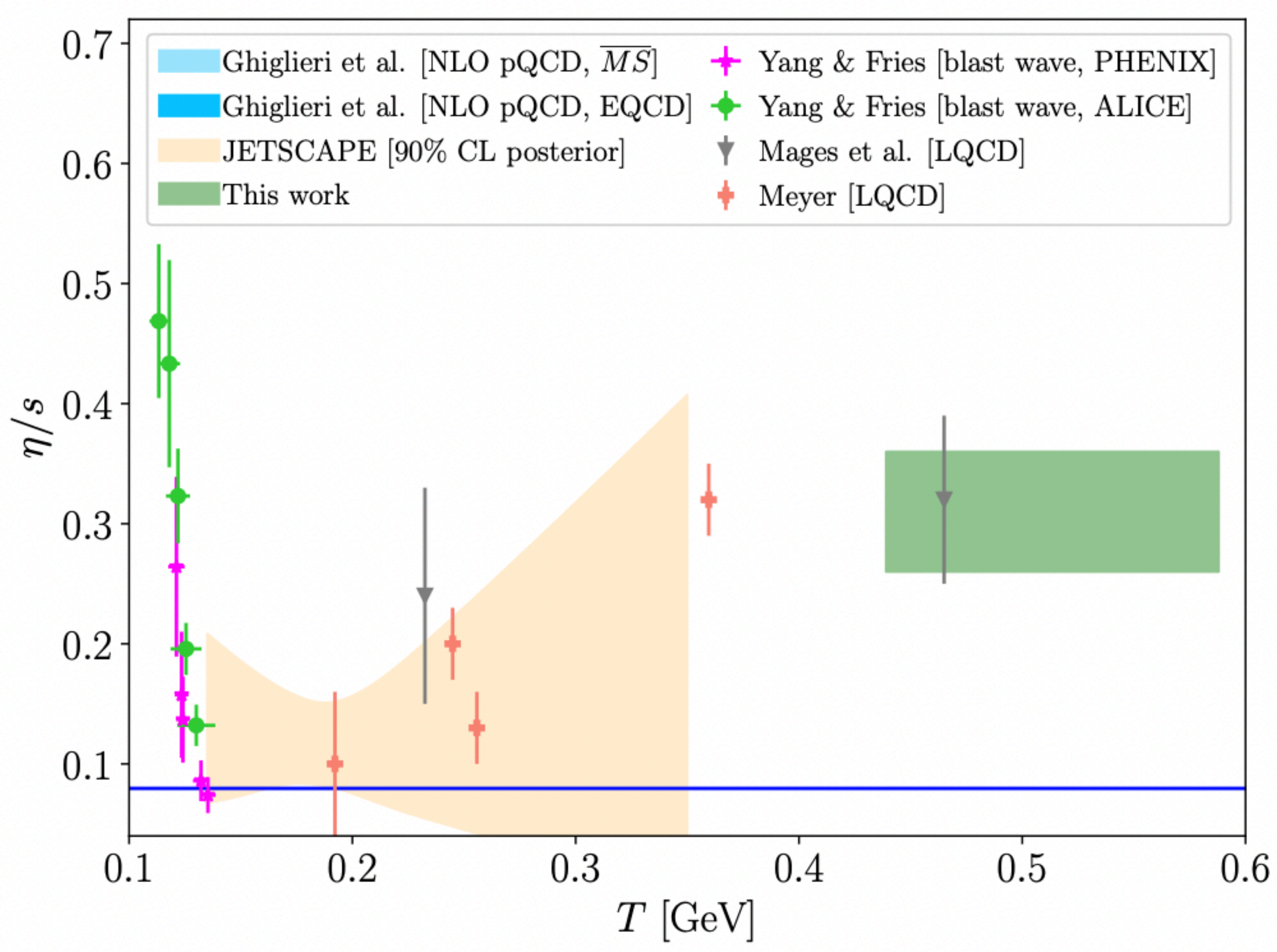

Constraints on the high-temperature shear-viscosity of QCD from constraint initial state & multiplicity measurements

``Constraining hot and cold nuclear matter properties from heavy-ion collisions and deep-inelastic scattering'' Andronic, Borghini, Du, Klein-Bösing, Krupczak, SS, arXiv:2504.02726

Conclusions

Developed simple hot-spot model that allows to simultaneously study cross-sections in e+A (mostly analytically) and eccentricities in p+A

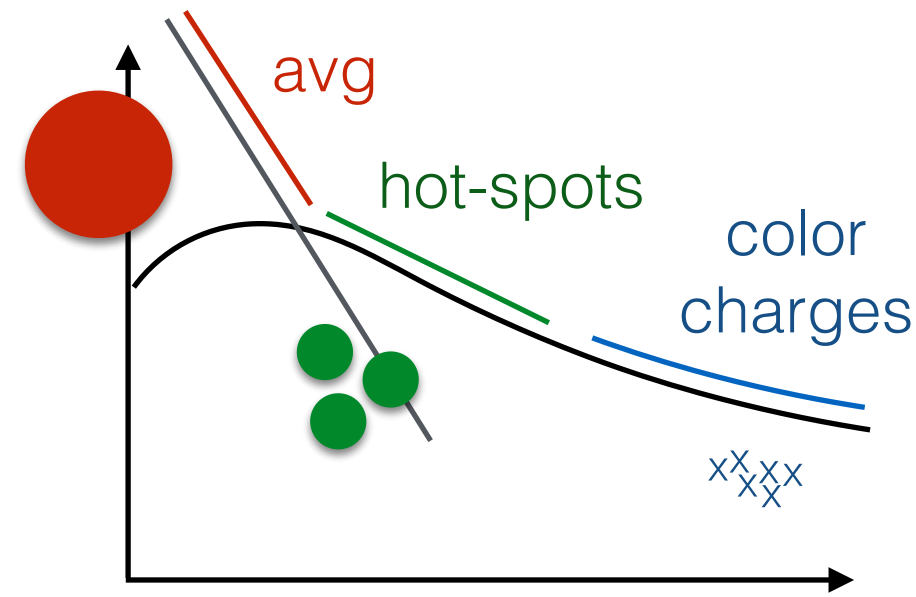

General anatomy of t-dependence of excl. VM cross-section clearly seen in HERA data

Structure of the probe more important than previously anticipated for J/ψ

-> Highly desirable to study cc and bb simultaneously to eliminate uncertainties from VM structure and truly access proton structure

-> Corrections to non-relativistic limit of VM wave-function improve agreement on HERA data

Global analysis from e+A to A+A promising to constrain cold and hot QCD properties simultaneously

Backup

Classification of contributions

Disconnected-Disconnected

$$\langle\alpha\alpha\alpha\alpha\rangle\langle\beta\beta\beta\beta\rangle = \langle\alpha\alpha\rangle\langle\alpha\alpha\rangle\langle\beta\beta\rangle\langle\beta\beta\rangle$$

proton fluctuations $+\langle\alpha\alpha\alpha\alpha\rangle_c\langle\beta\beta\rangle\langle\beta\beta\rangle$

nucleus fluctuations $+\langle\alpha\alpha\rangle\langle\alpha\alpha\rangle\langle\beta\beta\beta\beta\rangle_c$

$$+\langle\alpha\alpha\alpha\alpha\rangle_c\langle\beta\beta\beta\beta\rangle_c$$

combined fluctuations (neglected here)

Eccentricities in p+A collisions

Calculate correlation functions of energy density $\langle \epsilon(\mathbf{x}) \rangle, \langle \epsilon(\mathbf{x}) \epsilon(\mathbf{y}) \rangle$

Eccentricities
$$\varepsilon_n^{'}\{2\}^2_{\text{Approx}} = \frac{\int \mathrm{d}^2\mathbf{x}\mathrm{d}^2\mathbf{y}|\mathbf{x}-\mathbf{B}|^n|\mathbf{y}-\mathbf{B}|^n e^{in(\theta_{\mathbf{x}-\mathbf{B}}-\theta_{\mathbf{y}-\mathbf{B}})}\langle\varepsilon(\mathbf{x})\varepsilon(\mathbf{y})\rangle}{\int \mathrm{d}^2\mathbf{x}\mathrm{d}^2\mathbf{y}|\mathbf{x}-\mathbf{B}|^n|\mathbf{y}-\mathbf{B}|^n\langle\varepsilon(\mathbf{x})\rangle\langle\varepsilon(\mathbf{y})\rangle},$$

Distinguish between “proton”, “nucleus”contributions to correlation functions

$$\begin{aligned}
&\langle\varepsilon(\mathbf{x})\varepsilon(\mathbf{y})\rangle_{\mathrm{DC,C}} \\
&= \frac{Q_s^4 N^2}{4C_F^2}\int \mathrm{d}^2\mathbf{a}\mathrm{d}^2\mathbf{b}\Big[N_q F_2(\mathbf{a},\mathbf{b},\mathbf{B}) + N_q(N_q-1)F_3(\mathbf{a},\mathbf{b},\mathbf{B})\Big] \\
&\times\Big\{(N^2-1)^2\mathbf{G}^i_{\mathbf{x}}(\mathbf{x}-\mathbf{a})\mathbf{G}^i_{\mathbf{x}}(\mathbf{x}-\mathbf{a})\mathbf{G}^j_{\mathbf{y}}(\mathbf{y}-\mathbf{b})\mathbf{G}^j_{\mathbf{y}}(\mathbf{y}-\mathbf{b}) \\
&\qquad + 2(N^2-1)\mathbf{G}^i_{\mathbf{x}}(\mathbf{x}-\mathbf{a})\mathbf{G}^i_{\mathbf{x}}(\mathbf{x}-\mathbf{b})\mathbf{G}^j_{\mathbf{y}}(\mathbf{y}-\mathbf{a})\mathbf{G}^j_{\mathbf{y}}(\mathbf{y}-\mathbf{b})\Big\}
\end{aligned}$$

use homogenous nucleus in GBW model for simplicity
but include saturation on nuclear side

Eccentricities in p+A collisions

Energy fluctuations

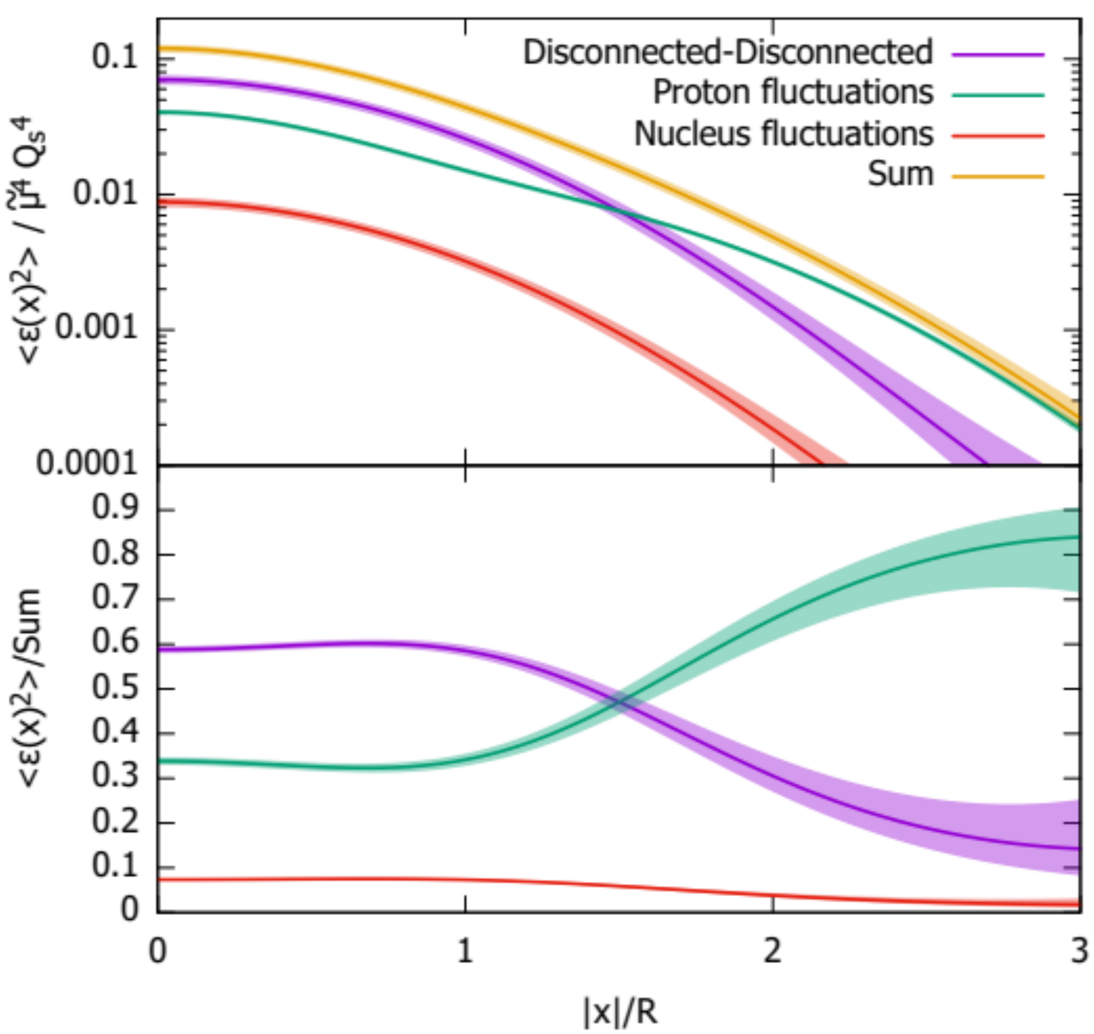

(a) $N_q = 3$

Energy-Energy correlator

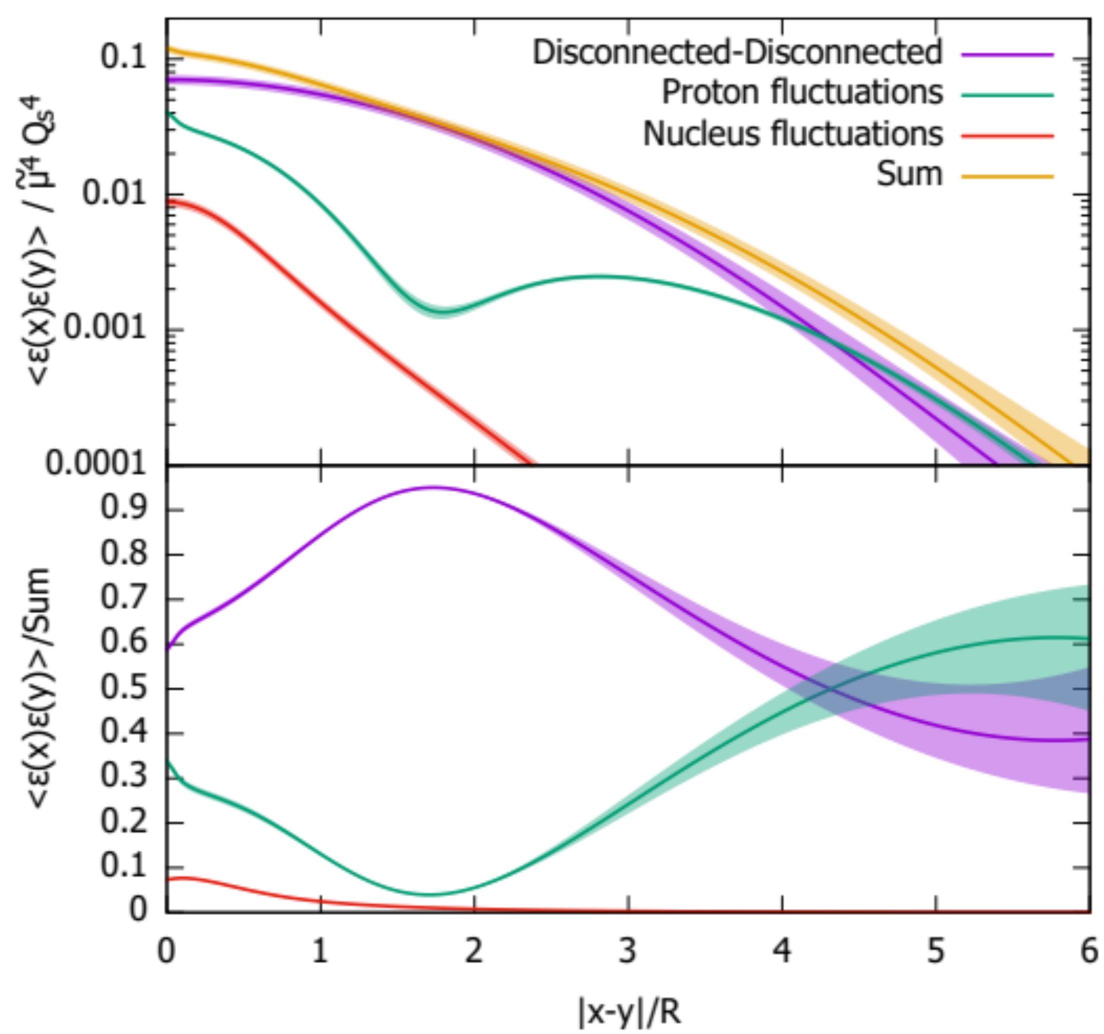

(b) $N_q = 3$

Verification that “proton shape” fluctuations dominate over nucleus fluctuations for typical scenarios of N_q~3 hot spots

Eccentricities in p+A collisions

Explicit verification that “proton shape” fluctuations dominate eccentricity

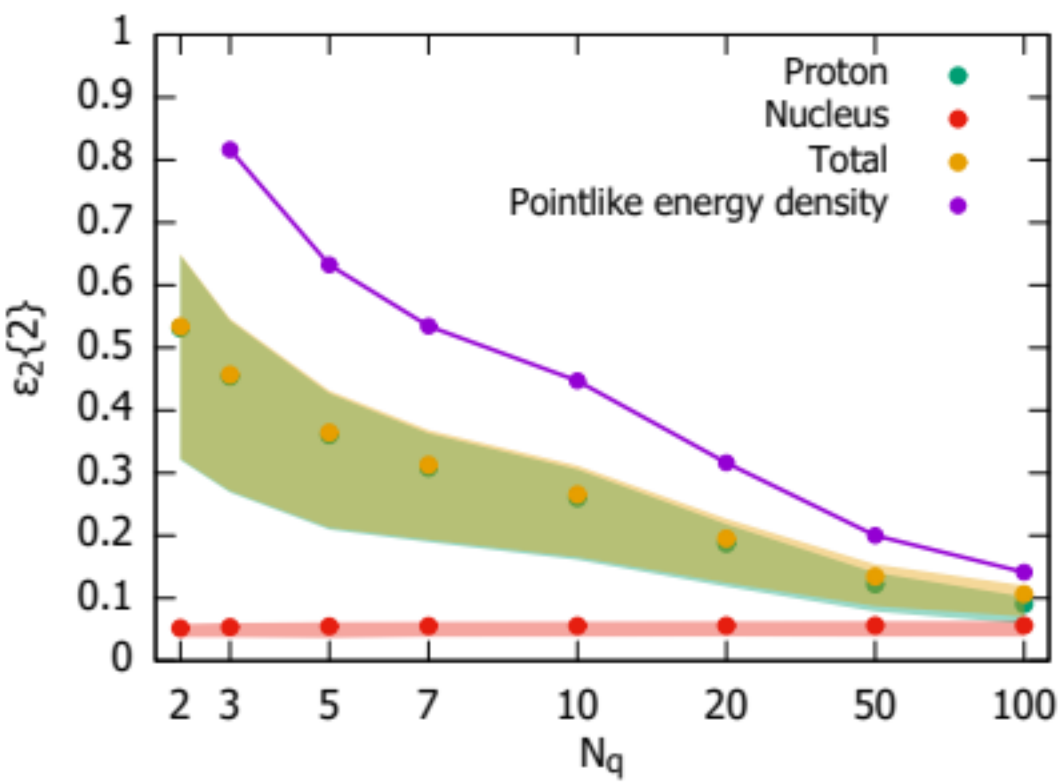

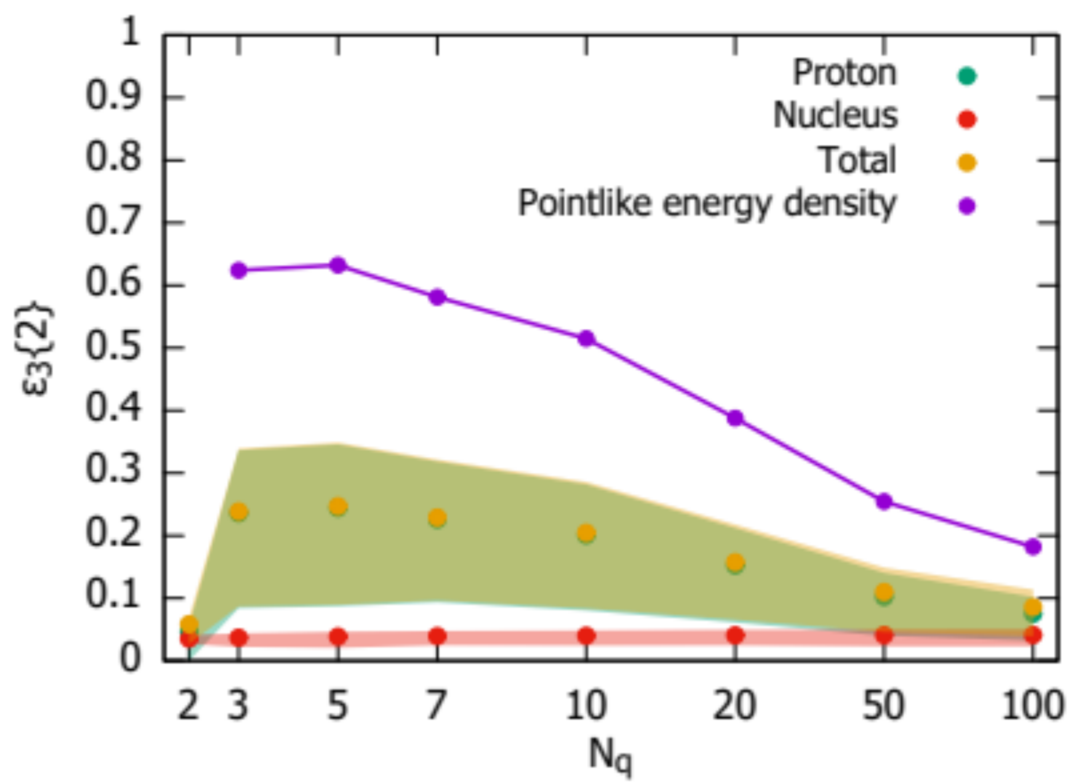

Strong sensitivity of eccentricities to

- IR regulator m (bands show 50% variations)
- Number of hot spots N_q